Biogeochemistry (2024) 167:251–267
https://doi.org/10.1007/s10533-024-01125-3

Disentangling the effects of temperature and reactive minerals on soil carbon stocks across a thermal gradient in a temperate native forest ecosystem

Idri Hastuty Siregar · Marta Camps-Arbestain · Gabor Kereszturi · Alan Palmer · Miko U. F. Kirschbaum · Tao Wang

Received: 11 May 2023 / Accepted: 29 January 2024 / Published online: 10 March 2024

Abstract Effects of global warming on soil organic carbon (C) can be investigated by comparing sites experiencing different temperatures. However, observations can be affected by covariance of temperature with other environmental properties. Here, we studied a thermal gradient in forest soils derived from volcanic materials on Mount Taranaki (New Zealand) to disentangle the effects of temperature and reactive minerals on soil organic C quantity and composition. We collected soils at four depths and four elevations with mean annual temperatures ranging from 7.3 to 10.5 °C. Soil C stocks were not significantly different across sites (average 162 MgC ha^{-1} to 85 cm depth, $P > .05$). Neither aluminium (Al)-complexed C, nor mineral-associated C changed significantly ($P > .05$) with temperature. The molecular characterisation of soil organic matter showed that plant-derived C declined with increasing temperature, while microbial-processed C increased. Accompanying these changes, soil short-range order (SRO) constituents (including allophane) generally increased with temperature. Results from structural equation modelling revealed that, although a warmer temperature tended to accelerate soil organic C decomposition as inferred from molecular fingerprints, it also exerted a positive effect on soil total C presumably by enhancing plant C input. Despite a close linkage between mineral-associated C and soil organic C, the increased abundance of reactive minerals at 30–85 cm depth with temperature did not increase soil organic C concentration at that depth. We therefore propose that fresh C inputs, rather than reactive minerals, mediate soil C responses to temperature across the thermal gradient of volcanic soils under humid-temperate climatic conditions.

Keywords Volcanic soil · Cross-site studies · Organo-mineral interactions · Organic matter composition

Responsible Editor: Samantha R Weintraub-Leff

Supplementary Information The online version contains supplementary material available at https://doi.org/10.1007/s10533-024-01125-3.

I. H. Siregar · M. Camps-Arbestain · G. Kereszturi · A. Palmer
School of Agriculture and Environment, Massey University, PB 11222, Palmerston North, New Zealand

M. U. F. Kirschbaum
Manaaki Whenua – Landcare Research, Private Bag 11052, Palmerston North 4442, New Zealand

T. Wang (✉)
CAS Key Laboratory of Mountain Surface Processes and Ecological Regulation, Institute of Mountain Hazards and Environment, Chinese Academy of Sciences, Chengdu 610041, China
e-mail: wangtao@imde.ac.cn

Introduction

The amount of organic C stored in the top 1 m of the world's soils is estimated to be around 1700 PgC, which is more than the C present in the atmosphere (~870 PgC) and terrestrial plants (~450 PgC) combined (IPCC 2021). One of the main factors affecting soil organic C dynamics is temperature (e.g., Kirschbaum 2000). Global warming may drive a net loss of soil C into the atmosphere (Keesstra et al. 2016), resulting in a positive terrestrial C–climate feedback loop (Crowther et al. 2016). Numerous mathematical models have projected a positive relationship between soil C loss and temperature, albeit with large uncertainty (Jones et al. 2005; Friedlingstein et al. 2006; Cox et al. 2013).

To reduce the uncertainty, there have been extensive experiments, including laboratory incubations and manipulated warming experiments, conducted to investigate the responses of soil organic C dynamics to temperature changes (Hicks Pries et al. 2017; Melillo et al. 2017; Li et al. 2020). However, previous warming experiments have primarily focused on soil C efflux and did not properly consider the effects of warming with concurrent changes in fresh C inputs. Fresh C inputs have been completely ignored in most laboratory incubations. While they are included in manipulated warming experiments, the general soil-only-warming approach cannot mimic the effect of whole-ecosystem warming on plant C inputs (Tian et al. 2023). Without a careful consideration of fresh C inputs, it is impossible to understand the warming effect on soil organic C pools that are determined by the balance between C outputs and inputs. Additionally, it is the soil organic C pools with a turnover time of decades to centuries that are more relevant to climate modelling (Trumbore and Czimczik 2008; Conant et al. 2011). However, most laboratory and field experiments are not run long enough for determining the long-term responses of soil organic C pools to warming. An approach to tackle the aforementioned problems regarding the insufficient considerations of fresh C inputs and experimental duration is to use cross-site studies that take advantage of natural thermal gradients along altitude gradients or over broad latitudinal scales (Carey et al. 2016; Xu et al. 2019). For instance, Giardina et al. (2014) investigated changes in soil organic C pools along a thermal gradient in a montane forest of Hawaii. They reported no significant effect of temperature on bulk soil organic C stocks, thus providing no evidence that a warmer temperature will have a direct impact on soil organic C stocks by accelerating soil organic C decomposition. However, one of the difficulties often encountered in studies of natural thermal gradient is that the temperature changes co-vary with various biotic and abiotic factors (Davidson and Janssens 2006; Carvalhais et al. 2014), including soil reactive minerals that also regulate soil organic C stocks and are also influenced by temperature, all of which confounds the response of soil organic C to warming (Doetterl et al. 2015). To use natural thermal gradients to fully understand the effects of long-term warming on soil organic carbon pools, it is, therefore, necessary to disentangle the interactive effects of temperature on soil reactive minerals and soil organic C concentration and composition.

A temperature gradient on the side of the dormant volcano, Mt. Taranaki, in New Zealand provides an excellent natural laboratory to study the effects of mean annual temperature (MAT), which changes by around 3.2 °C along an elevation gradient ranging from 512 to 1024 m above sea level (asl), with a relatively uniform parent material and native vegetation cover. Precipitation is > 3000 mm $year^{-1}$, with regular rainfall throughout the year, thus not limiting either vegetation growth or mineral weathering. The soils along the thermal gradient are Andosols, which predominantly contain reactive Al and Fe in the form of organo-Al complexes and/or SRO constituents (e.g., allophane, imogolite and ferrihydrite) (Masiello et al. 2004; Takahashi and Dahlgren 2016), onto which organic ligands can attach and become protected from decomposition (Yuan et al. 2000; Hashizume and Theng 2007; Parfitt 2009). Elevated temperature, under high rainfall and good drainage, increases the rate of physical and chemical weathering of the volcanic parent material, which is key in enhancing the formation of reactive Al and Fe that in turn influences soil organic C persistence by forming organo-Al complexes and organo-SRO associations (Macías and Camps-Arbestain 2020; Lawrence et al. 2021). However, it remains unclear how temperature influences the relative abundance of the different forms of reactive Al/Fe and, in turn, the mechanisms of C protection. Although there seems to be a mismatch in response rates of mineral weathering and organic C

accumulation to temperature, the formation of reactive mineral from volcanic materials is rapid under warm and humid conditions (Anda et al. 2023), which is thus relevant to study the response of soil C storage to climate change.

This study thus aims to disentangle the influences of temperature, soil reactive minerals and their interactions on soil organic C stocks and composition across the thermal gradient of Mt. Taranaki. We hypothesised that: (i) the presence of SRO differs along the thermal gradient, with a greater abundance at warmer sites (i.e., lower altitudes), where the weathering rate is faster leading to greater supply of hydroxyl ions (OH^-) (Delmelle et al. 2015). Under such conditions, OH^- are able to compete with organic ligands for Al, favouring the formation of the SRO constituents over that of organo-Al complexes (Mizota and van Reeuwijk 1989; Dahlgren et al. 2004); (ii) under warmer conditions, soil organic C is likely to be more microbially processed than under colder conditions where chemical composition of organic matter more closely resembles the chemical composition of the source plant material; and as a result, (iii) the mechanisms of C protection along the transect differ, with more C being associated with minerals at warmer sites.

Material and methods

Site description

The study was conducted in a mature native forest on the eastern flank of Mt. Taranaki in the North Island of New Zealand. Four sampling sites were chosen, with elevations at 512, 680, 880 and 1024 m asl. Mean annual temperature (MAT) at the four elevations were 10.5 °C (abbreviated as T10), 9.1 °C (T9), 8.2 °C (T8), and 7.3 °C (T7), and mean annual precipitation rates exceeded 3000 mm per year at all sampling sites. Details of the elevation, GPS coordinates, MAT, and mean annual precipitation are provided in supporting information, Fig. S1 and Table S1. All sampling sites had non-limiting plant-available moisture, and similar native evergreen broadleaf trees (> 80% kamahi (*Weinmannia racemosa* L.f.) and mahoe (*Melicytus ramiflorus* J.R & G. Forster). The soil was formed on andesitic tephra of the Burrell formation deposited in A.D. 1655 (Aitken et al. 1978; Torres-Orozco et al. 2017) and is classified as an alu-andic Andosol according to the World Reference Base system (World Reference Base for Soil Resources 2015). The topography ranges from gentle to steep (Davies and Lambert 2015), but all sampling sites were located away from streams and gullies to minimise the effects of erosion. The forest is assumed to be in a steady-state condition in terms of soil organic C storage after a series of successional stages from shrubs to the current native forest initiated after the latest eruption in A.D. 1655 (McGlone et al. 1988; Clarkson 1990). Mt. Taranaki's most recent activity occurred between 1785 and 1820, erupted on the northwestern slopes, and had minor effect on these sampling sites (Platz et al., 2012). No studies have documented any major damage caused by natural or human disturbance that would have resulted in significant changes to the forest's structure.

Soil sampling and reactive mineral extraction

Soil samples were taken with a 25-mm diameter soil corer at four different depths (0–10, 10–30, 30–50, and 50–85 cm) with four replicates per elevation (within an area of ~ 400 m^2). Soil bulk density was determined by dividing the soil's dry weight by the volume of the soil core. The soil samples were air-dried, sieved (< 2-mm) and analysed for pH (soil/deionised water = 1/2.5, w/v), sodium pyrophosphate-extractable Al (Al_{py}) and iron (Fe_{py}), and oxalate-extractable Al (Al_{ox}), iron (Fe_{ox}) and silicon (Si_{ox}). Fe_{py} and Al_{py} were extracted using 0.1 M sodium pyrophosphate ($Na_4P_2O_7$; pH ~ 10) as described by Blakemore et al. (1981). Note that Fe_{py} contains ferrihydrite, therefore should not be exclusively considered as organo-chelated Fe. Al_{ox}, Fe_{ox} and Si_{ox} were extracted by 0.1 M acid ammonium oxalate (pH = 3) in a dark room following the method of Blakemore et al. (1981). These values were used to estimate the quantity of SRO constituents, including allophane content, which was estimated following the method of Mizota & Van Reeuwijk (1989) using Si_{ox}, Al_{ox}, and Al_{py} values. The concentrations of Al, Fe, and Si in all extractants were determined using a microwave plasma-atomic emission spectrometer (4200 MP-AES, Agilent Technologies, Singapore). More details are provided in the supporting materials and methods.

Total C and nitrogen contents and stocks

Total C and total nitrogen (N) contents were analysed with an Elementar (Vario MACRO, Hanau, Germany). Total soil organic C stocks at fixed depths were calculated by considering the soil organic C content, soil bulk density, and soil depth. Because of the presence of lapilli material (2–64 mm in diameter), particularly at sites T7 and T8 at depths of 30–50 and 50–85 cm, the total soil organic C stocks at these depths were calculated after correction for the coarse fragments, following Schwager & Mikhailova (2002) as follows:

$$TC_{s\_i} = TC_i \times \rho_i \times D_i \times \left(1 - \delta_{2mm\_i}\right) \times 0.1 \quad (1)$$

where TC_{s_i} represents the C stocks (Mg ha^{-1}), ρ_i the soil bulk density (g cm^{-3}), D_i the thickness of soil layers (cm), and δ_{2mm_i} the proportion of the coarse fragments on a volume basis (> 2-mm mesh) (%) of a specific soil layer *i*. The soil organic C stocks at 0–10, 0–30, 0–50, and 0–85 cm (Mg ha^{-1} 0.10 m^{-1}, Mg ha^{-1} 0.30 m^{-1}, Mg ha^{-1} 0.50 m^{-1}, Mg ha^{-1} 0.85 m^{-1}) were estimated on the basis of an equivalent soil mass, following Wendt and Hauser (2013).

Metal-complexed and SRO constituents-associated C

Metal-complexed C (C_{py}) was extracted using 0.1 M sodium pyrophosphate. The details are provided in the supporting materials and methods S1.3. In the pH range (4.8–5.7, Fig. S2) of the soils under study, C_{py} was considered to mostly consist of organo-Al complexes (Dahlgren et al. 1993; Shen et al. 2018). Mineral-associated C was indicated by hydrofluoric acid (HF) treatment (Eusterhues et al. 2007) following a method slightly modified from Wang et al. (2016). Briefly, air-dried soil (< 2-mm) was washed with 2% HF for 8 h per cycle and repeated for 8 cycles. The washed soil residues were collected by centrifugation and dried at 45 °C. The dried residues were weighed, ground to < 100 µm and analysed for C and N contents on Elementar. The C recovered in each soil residue after the HF treatment was then calculated. The C fraction mobilised by 2% HF ($C_{HF\text{-}mob}$) was calculated as C loss during the HF treatment. It should be noted that, although only a part of C that associates with minerals is removed by HF treatment, $C_{HF\text{-}mob}$ is a good indicator of the extent of C that interacts with SRO constituents and minerals (Eusterhues et al. 2003; Rumpel et al. 2008).

Soil organic composition

Soil organic C composition of HF-treated soil was identified by pyrolysis–gas chromatography–mass spectrometry (Py-GC/MS) following Wang et al. (2016). The use of HF-treated soil was aimed to reduce the interference of soil reactive mineral constituents with the pyrolysis reactions of soil organic matter (Zegouagh et al. 2004). The Py-GC/MS instrument comprised a Multi-Shot Pyrolyser (EGA/PY-3030D, Frontier Lab, Fukushima, Japan) connected to a GC/MS unit (GCMS QP2010 Ultra, Shimadzu, Kyoto, Japan). ~ 0.5 to 3 mg of each soil (depending on its C content) was pyrolysed at 550 °C for 12 s. The injection was carried out in a split mode (split ratio: 1:30). The pyrolysis products were separated on a stainless-steel capillary column (SH-Rxi-5 ms Crossbond, Shimadzu; 5% diphenyl/95% dimethyl poly siloxane, 30 m, 0.25 mm internal diameter, with a film thickness of 0.50 µm). High-purity helium was used as a carrier gas with a flow rate of 1 mL min^{-1}. The initial oven temperature was 40 °C, which was maintained for 12 s (the same as the pyrolysis time) and then amplified up to 300 °C at a rate of 5 °C min^{-1}. The final column temperature was 300 °C and was maintained for 16 min. The interface temperature of GC/MS was 270 °C, and the ion source temperature was 230 °C. The ionisation energy was set to 70 eV, with a m/z range of 45–650 and a cycle time 0.5 s. In total, 109 peaks were identified by GC/MS solution software (Shimadzu) according to the NIST library and published sources such as Buurman et al. (2007), Suárez-Abelenda et al. (2015), and Wang et al. (2016). The relative abundance of each pyrolysis product was calculated by normalising the peak area of its primary fragment ion(s) to the sum of the total quantified peak area (TQPA). The pyrolysis products were grouped into the following compound classes: carbohydrates, methylene chain compounds, lignin-derived compounds, monocyclic aromatic hydrocarbons (MAHs), polycyclic aromatic hydrocarbons (PAHs), N-bearing compounds, and other compounds (Shen et al. 2018).

Data analysis

Statistical analysis of the major soil properties was carried out with IBM SPSS Statistics version 25.0 (IBM Corp., Armonk, New York, USA). One-way ANOVA with Tukey's test was performed to assess significant differences (at $P < 0.05$) between means. Two-way ANOVA were conducted to examine the effects of MAT, soil depth and their interactions on soil reactive Al and Fe and C properties. Linear regression was used to assess (i) the temperature trend of soil reactive Al and Fe species, total C and its fractions and pyrolysis products, and (ii) the correlation between reactive Al/Fe and the total C and C fractions. A principal component analysis (PCA) was performed to separately examine the relationships between soil total C and its fractions, with either soil properties or organic composition. Prior to conducting the PCA, the soil properties (including the different C fractions) were normalised to z-scores to avoid scaling effects. Structural equation modelling (IBM SPSS-Amos 25.0) was used to disentangle the direct and indirect effects of MAT and soil reactive Al/Fe on soil total C concentrations. Soil reactive minerals, organic composition, and SRO constituents-associated C were used as latent variables. Principal Component (PC) 1 loadings of extractable cations, SRO constituents and allophane content and of pyrolysis product groups were used as indicators of soil reactive minerals and organic composition, respectively.

Results

Soil chemical properties

Soil chemical properties co-varied with temperature across the elevational gradient of Mt Taranaki. Soil pH generally increased with temperature at any specific soil depth, although the difference was only significant at the 10–50 cm depth, between T10 and both T7 and T8 ($P < 0.05$, Fig. S2). Across the transect, the soil at 0–10 cm had a significantly lower pH than at the deepest soil layer ($P < 0.05$), except for T10. Total reactive Al (Al_{ox}) also tended to increase with temperature for all soil depths except 10–30 cm. In particular, T10 soil had significantly higher Al_{ox} values than soils from sites with lower temperatures ($P < 0.05$; Fig. 1a). Fe_{ox} showed similar patterns with elevation and depth as observed for Al_{ox} (Fig. 1b). As a result, SRO constituents ($Al_{ox} + ½Fe_{ox}$) also displayed a similar trend to Al_{ox} (Fig. 1c). Allophane contents were almost negligible at soil depths of less than 30 cm at almost all sites except T10 but increased with temperature and depth (Fig. 1d). Site T10 had the highest allophane content across the thermal gradient, although significant differences between T7 and T10 were only detected at the 30–85 cm soil depth. There were no consistent trends in organo-complexed Al (Al_{py}) (Fig. 1e) and pyrophosphate extractable Fe (Fe_{py}) across the thermal gradient (Fig. S3a). At each site, both Al_{py} and Fe_{py} showed unimodal trends along the soil profile, with maximum values observed at 10–30 cm and minima at 0–10 cm. Al_{py} showed a good correlation with Fe_{py}, with the molar concentration of Fe_{py} being ca 27% of that of Al_{py} (Fig. S3b). Moreover, the Al_{py}/Al_{ox} ratio tended to decrease with increasing temperature and soil depth (Fig. 1f).

Soil C contents, stocks and C:N ratios

Overall, at any specific depth, total C content did not show any consistent trend as a function of temperature (Fig. 2). At 0–10 cm and 30–50 cm soil depths, there were no significant differences in total C between sites ($P > 0.05$). By contrast, at 10–30 cm, T7 and T8 had significantly higher total C than the warmer sites ($P < 0.05$). At the 50–85 cm depth, T8 and T10 had a significantly larger total C content than T7 and T9 ($P < 0.05$). Consequently, cumulative soil organic C stocks down to 85 cm across the thermal gradient were not significantly different ($P > 0.05$, Fig. S4).

Soil C fractions associated with metal cations and SRO constituents

The relative importance of organic C that forms complexes with metal cations versus that associated with reactive minerals were evaluated by calculating the ratio of C_{py} to $C_{HF\text{-}mob}$ ($C_{py}/C_{HF\text{-}mob}$). C_{py} did not differ among sites at any specific soil depth, except at T9 at 10–30 cm and 50–85 cm where values were significantly lower than at other sites (Fig. S5). Normalised to total C, there was no significant difference in C_{py} either among sites or across soil depths ($P > 0.05$; Fig. 3a). Although there were no significant changes in $C_{HF\text{-}mob}$ across the thermal gradient (except at

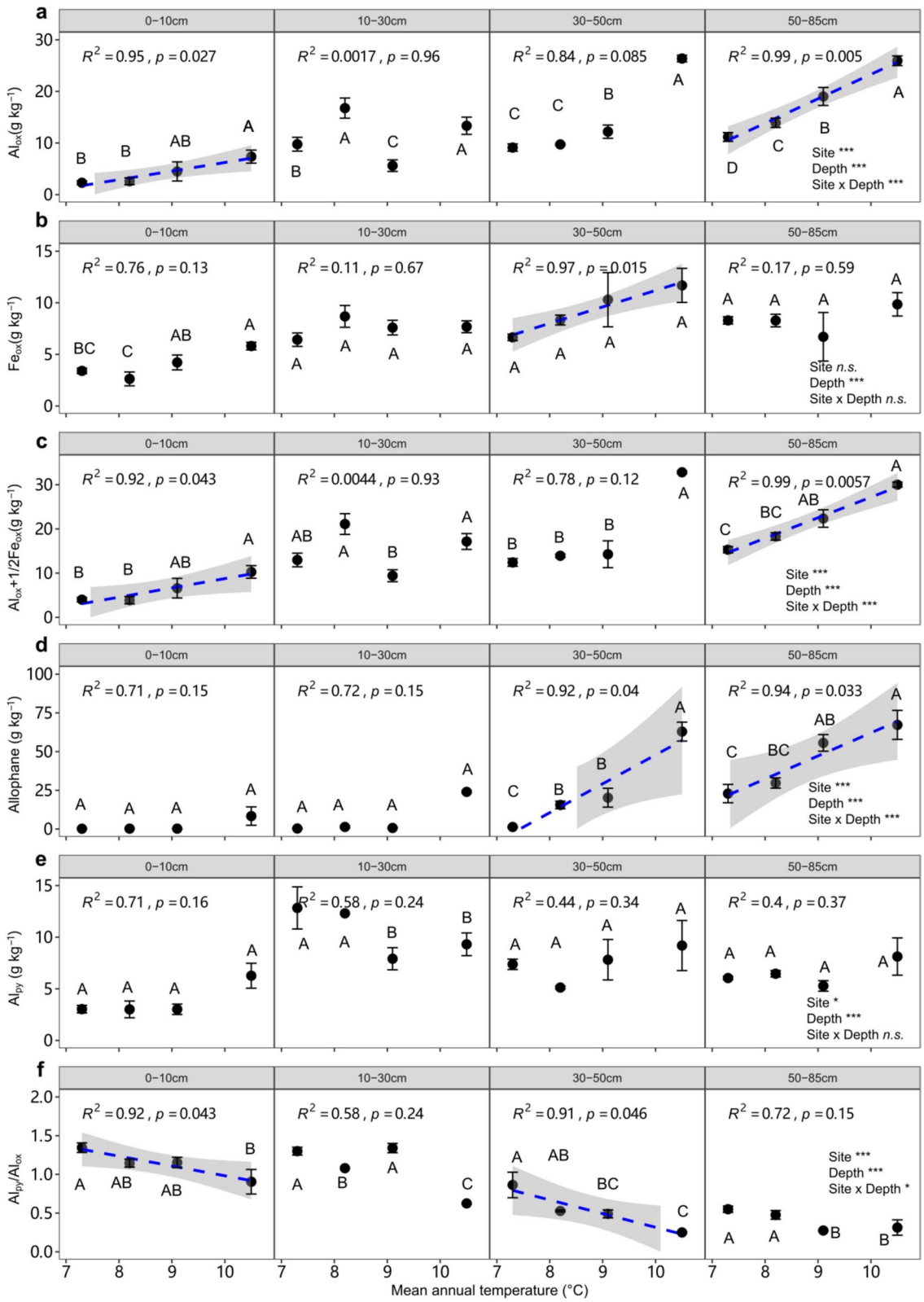
a
0–10cm
10–30cm
30–50cm
50–85cm
Al_{ox}(g kg^{-1})
R^2 = 0.95 , p = 0.027
R^2 = 0.0017 , p = 0.96
R^2 = 0.84 , p = 0.085
R^2 = 0.99 , p = 0.005
Site ***
Depth ***
Site x Depth ***
b
Fe_{ox}(g kg^{-1})
R^2 = 0.76 , p = 0.13
R^2 = 0.11 , p = 0.67
R^2 = 0.97 , p = 0.015
R^2 = 0.17 , p = 0.59
Site n.s.
Depth ***
Site x Depth n.s.
c
Al_{ox}+1/2Fe_{ox}(g kg^{-1})
R^2 = 0.92 , p = 0.043
R^2 = 0.0044 , p = 0.93
R^2 = 0.78 , p = 0.12
R^2 = 0.99 , p = 0.0057
Site ***
Depth ***
Site x Depth ***
d
Allophane (g kg^{-1})
R^2 = 0.71 , p = 0.15
R^2 = 0.72 , p = 0.15
R^2 = 0.92 , p = 0.04
R^2 = 0.94 , p = 0.033
Site ***
Depth ***
Site x Depth ***
e
Al_{py} (g kg^{-1})
R^2 = 0.71 , p = 0.16
R^2 = 0.58 , p = 0.24
R^2 = 0.44 , p = 0.34
R^2 = 0.4 , p = 0.37
Site *
Depth ***
Site x Depth n.s.
f
Al_{py}/Al_{ox}
R^2 = 0.92 , p = 0.043
R^2 = 0.58 , p = 0.24
R^2 = 0.91 , p = 0.046
R^2 = 0.72 , p = 0.15
Site ***
Depth ***
Site x Depth *
Mean annual temperature (°C)

◂**Fig. 1** Reactive Al and Fe species of forest soils across a thermal gradient on Mt. Taranaki. **a**, **b** and **c** Al_{ox}, Fe_{ox} and short-range order (SRO) constituent contents, respectively; **d** allophane content; **e** Al_{py} content and **f** Al_{py}/Al_{ox} ratio. Different capital letters adjacent to dots denote a significant difference among the four mean annual temperatures (MAT) at the same depth according to one-way ANOVA followed by Tukey's test ($P < 0.05$). Two-way ANOVA results with both MAT and depth as covariates are shown on the rightmost panel, with asterisks indicating significant (*$P < 0.05$; **$P < 0.01$, ***$P < 0.001$, and *n.s.* nonsignificant). Error bars represent the standard error of the means (n = 4). Results of linear regressions (y variable ~ mean annual temperature at the same depth) are shown on the top of each panel and fitted lines with a 95% confidence band are shown if the regression is significant ($P < 0.05$). Abbreviations: Al_{ox} and Fe_{ox} oxalate-extractable Al and Fe; Al_{py} sodium pyrophosphate-extractable Al

50–85 cm where the value of T10 was higher than T7 and T9, Fig. S5b), total C-normalised $C_{HF\text{-}mob}$ tended to increase with temperature and soil depth and the values were significantly different between T7 and T10 ($P < 0.05$; Fig. 3b). The C_{py} to $C_{HF\text{-}mob}$ ratio did not differ significantly across the thermal gradient ($P > 0.05$) (Fig. 3c).

Soil organic composition by Py-GC/MS

Among the different groups of compounds identified by Py-GC/MS, carbohydrates, lignin and MAHs had the most distinct patterns across the temperature gradient (Fig. 4). Methylene chain compounds (MCCs), PAHs, N-derived and other compounds did not show a consistent pattern across the thermal gradient.

Carbohydrates were the relatively most abundant group among all identified pyrolysis product groups, accounting for 40–65% of TQPA (Fig. 4a). Identified carbohydrate compounds included acetic acid, furans, furaldehydes, cyclopentenones, 4-hydroxy-5,6-dihydro-(2*H*)-pyran-2-one, and levoglucosan (Table S2). A clear decrease in the relative abundance of carbohydrates and plant-derived carbohydrate biomarkers (e.g. levoglucosan) as temperature increased was observed at all soil depths. The relative abundance of carbohydrates also decreased with depth.

The pyrolysis products of lignin (4-vinylphenol, guaiacols, and syringols) accounted for 4–13% of TQPA (Fig. 4b). Unlike carbohydrates, the contribution of lignin tended to increase with temperature (significant $P < 0.05$ between T7 and T10 at depths of 0–10 and 50–85 cm). However, their abundance tended to decrease with increasing soil depths.

Nitrogen-bearing compounds (e.g., pyrrole, pyridine, acetamide, and diketopiperazines) accounted for 4–7% of the TQPA (Fig. 4c). The relative abundance of N compounds was not significantly different ($P > 0.05$) across the thermal gradient. At each site, the relative abundance of N compounds was highest at the 10–30 cm depth and lowest at 0–10 cm.

Monocyclic aromatic hydrocarbons (e.g., benzene and methylbenzenes) accounted for 5–11% of TQPA (Fig. 4d). Apart from the lack of a clear trend in the 0–10 cm soil depth, MAHs tended to increase with temperature at other soil depths. This group also tended to increase with soil depths.

Methylene chain compounds (e.g., alkanes, alkenes, and fatty acids) contributed to 12–37% of TQPA, being the second largest among all identified pyrolysis product groups (Fig. 4e). There were no consistent patterns of methylene chain compounds with temperature, but their abundance tended to increase with soil depths. PAHs comprised < 1% of TQPA and were not significantly different across the thermal gradient (Fig. 4f; $P > 0.05$).

Relationships between soil organic C and either soil chemical properties or organic composition

PCA was first performed on soil chemical properties (e.g., various extractable cations, pH, Olsen P and C/N) and total C and its fractions (i.e., absolute and total C normalized $C_{HF\text{-}mob}$, and C_{py}) at all soil depths across the thermal gradient to explore how soil organic C contents and soil chemical properties varied with temperature and soil depth. The first two PCs accounted for 59% of the variability, with PC1 accounting for 44% of the variability and PC2 for 15% (Fig. 5a). The positive loading of PC1 was generally driven by high pH, Al_{ox}, Fe_{ox}, Si_{ox}, allophane, and SRO constituents, and the negative side by Al_{py}/Al_{ox}. PC2 was driven by the presence of Al_{py}, Fe_{py} and the C/N ratio. Total C, total N, and Olsen-P were associated with large Al_{py}/Al_{ox} values, plotting away from high pH values, allophane and SRO constituents. Total C was closely associated with C_{py}, and to a lesser extent with C_{HF_mob}, while total C-normalised C_{HF_mob} was positioned away from total C. MAT was plotted in the fourth quadrant, showing a weak positive correlation with allophane contents, while it

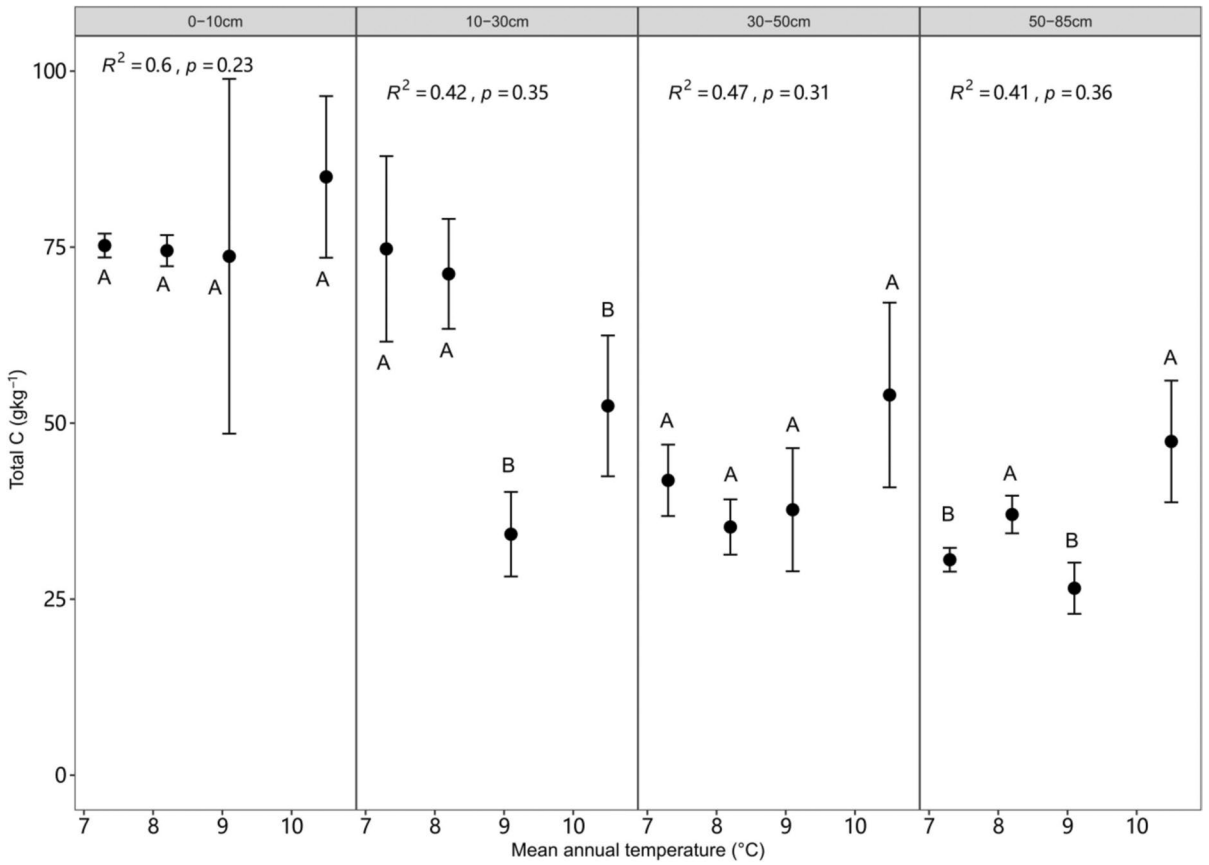

Fig. 2 Total C contents in forest soils across the thermal gradient. See Fig. 1 for explanations of labels

showed a weak negative correlation with total C and the C fractions. Soil depth were plotted on the positive axis of PC1 and tightly associated with pH, allophane, Si_{ox}, and total C-normalised $C_{HF\text{-}mob}$, and away from total C.

The relationships among soil organic composition, total C and its fractions across the thermal gradient were also examined using PCA to reveal how soil organic composition covaried with temperature and soil depth and how it is associated with soil organic C contents. The first two PCs accounted for 61% of the variability, with PC1 accounting for 44% of the variability and PC2 17% (Fig. 5b). The positive side of PC1 was driven by lignin and carbohydrates, while the negative side was contributed largely by methylene chain compounds, MAHs and PAHs. PC2 was positively correlated with C/N ratios and carbohydrates, and negatively correlated with N compounds, MAHs and lignin. Total C, C_{py}, and $C_{HF\text{-}mob}$ plotted close to carbohydrates and away from methylene chain compounds. This contrasts with total C-normalised $C_{HF\text{-}mob}$ as this plotted close to methylene chain compounds, and away from lignin and carbohydrates. Soil depth was plotted on the negative PC1 axis, displaying a positive relationship with methylene chain compounds and a negative relationship with lignin and carbohydrates. MAT, on the other hand, was placed on the negative PC2 axis, showing positive relationships with N compounds, lignin and MAHs and negative with C/N and $C_{HF\text{-}mob}$ and, to a lesser extent, with carbohydrates. These results suggested enhanced preservation of plant-derived polysaccharides when temperatures were low and preferential decomposition of these polysaccharides, and the enrichment of microbial-derived compounds (e.g., N compounds), lignin and MAHs, when temperatures were higher.

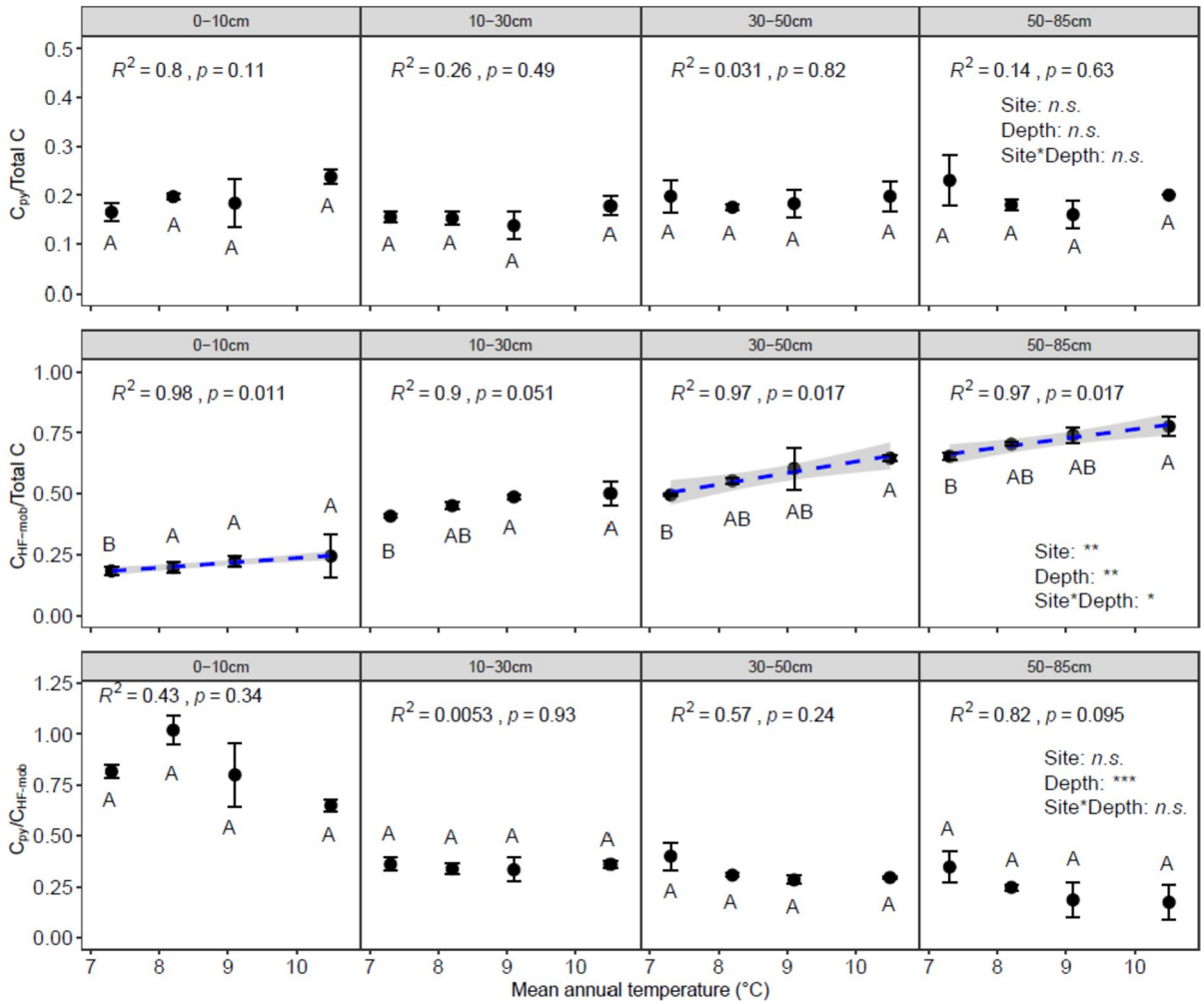

Fig. 3 Extractable soil organic C fractions across the thermal gradient. **a** Pyrophosphate-extractable C normalized to total C (C_{py}/total C); **b** Hydrofluoric acid-extractable C normalized to total C ($C_{HF\text{-}mob}$/total C) and their ratios **c**. See Fig. 1 for explanations of labels

Structural equation modelling was used to disentangle the direct and indirect effects of temperature and reactive minerals on total soil organic C contents (Fig. 6). Incorporating data from all soil depths into the analysis, we found that 89% of the variability of total C contents could be explained by MAT, depth, organic composition, reactive Al and Fe species and mineral-associated C (inferred from $C_{HF\text{-}mob}$). Mineral-associated C had a direct positive on total C contents, while reactive Al and Fe species had a weak direct negative effect. Other variables, including soil organic composition (mainly contributed by N compounds, PAHs and methylene chain compounds) did not have any significant direct effects on total C. Both MAT and soil depth had indirect effects on total C via their effects on mineral-associated C.

As the effects of temperature were intermingled with those of soil depth, structural equation modelling was also performed separately for each depth. The selected variables (MAT, organic composition, reactive minerals, and mineral-associated C) explained over 96% of the variability of total C at each soil depth. Mineral-associated C still manifested the strongest direct effect on total C, irrespective of soil depth. In contrast to the lack of effects across the whole soil profile, soil organic matter composition

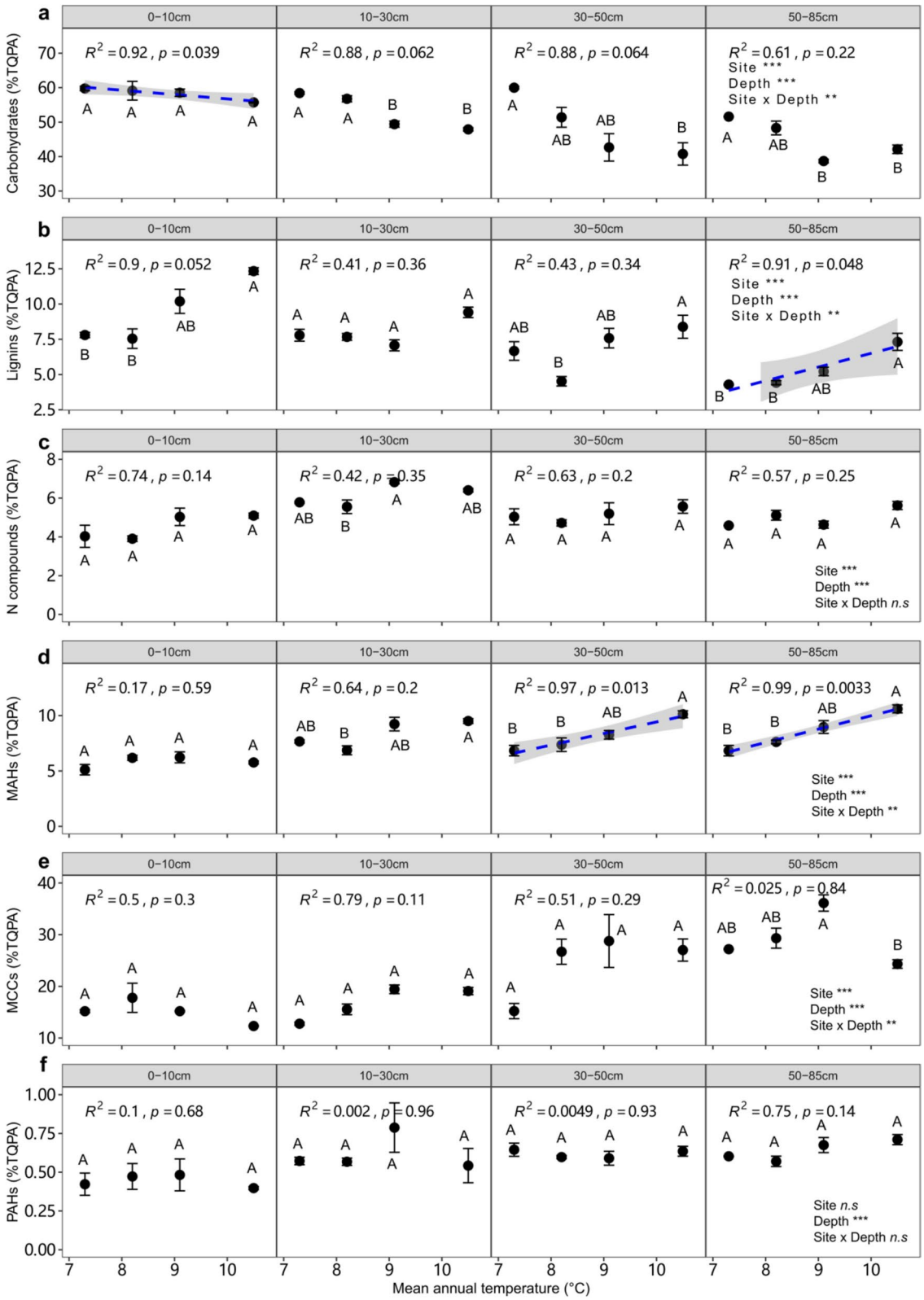
a
0–10cm
10–30cm
30–50cm
50–85cm
Carbohydrates (%TQPA)
R² = 0.92 , p = 0.039
R² = 0.88 , p = 0.062
R² = 0.88 , p = 0.064
R² = 0.61 , p = 0.22
Site ***
Depth ***
Site x Depth **
b
Lignins (%TQPA)
R² = 0.9 , p = 0.052
R² = 0.41 , p = 0.36
R² = 0.43 , p = 0.34
R² = 0.91 , p = 0.048
Site ***
Depth ***
Site x Depth **
c
N compounds (%TQPA)
R² = 0.74 , p = 0.14
R² = 0.42 , p = 0.35
R² = 0.63 , p = 0.2
R² = 0.57 , p = 0.25
Site ***
Depth ***
Site x Depth n.s
d
MAHs (%TQPA)
R² = 0.17 , p = 0.59
R² = 0.64 , p = 0.2
R² = 0.97 , p = 0.013
R² = 0.99 , p = 0.0033
Site ***
Depth ***
Site x Depth **
e
MCCs (%TQPA)
R² = 0.5 , p = 0.3
R² = 0.79 , p = 0.11
R² = 0.51 , p = 0.29
R² = 0.025 , p = 0.84
Site ***
Depth ***
Site x Depth **
f
PAHs (%TQPA)
R² = 0.1 , p = 0.68
R² = 0.002 , p = 0.96
R² = 0.0049 , p = 0.93
R² = 0.75 , p = 0.14
Site n.s
Depth ***
Site x Depth n.s
Mean annual temperature (°C)

◂**Fig. 4** Relative abundances (%TQPA) of pyrolysis product groups in forest soils across the thermal gradient. **a** carbohydrates, **b** lignin-derived compounds, **c** N-bearing compounds, **d** monocyclic aromatic hydrocarbons (MAHs), **e** methylene chain compounds (MCCs), and **f** polycyclic aromatic hydrocarbons (PAHs), respectively. Other pyrolysis products are not shown due to their lack of consistent patterns across either sites or soil depths. See Fig. 1 for explanations of labels

showed a direct effect on total C at any specific soil depth. In addition, the effect of organic composition changed gradually from a weak positive to a strong negative effect as soil depth increased. Both MAT and reactive minerals had direct effects on total C contents at the 30–50 and 50–85 cm soil depths, while no significant direct effect was observed at the 0–30 cm soil depth. MAT also indirectly influenced total soil organic C contents through its effect on soil organic matter composition at depth. By contrast, reactive minerals showed an indirect effect on total C contents by influencing mineral-associated C at the 0–30 cm depth only. Notably, MAT directly influenced reactive minerals consistently across the soil profile.

Discussion

Temperature influences reactive minerals by enhancing weathering

The observation that SRO constituents increased with increasing temperature (Fig. 1) supports the first hypothesis that SRO constituents are more abundant at warmer sites. The study also reveals that (i) with increasing temperature, the relative importance of the organo-Al complexes versus SRO constituents decreased with increasing temperature, as assessed by the reduced Al_{py}/Al_{ox} ratios, and (ii) with increasing soil depth, SRO constituents increased and Al_{py}/Al_{ox} ratios decreased. Such trends were paralleled by an increase in soil pH (Fig. S2). This can be explained by the fact that (i) warmer temperatures accelerate mineral weathering (and thus the generation of OH^-); and (ii) at deeper soil layers, the lower amounts of organic acidity are less able to balance the OH^- generated (Macías and Camps-Arbestain 2020). Moreover, as the concentration of OH^- increases, these anions preferably bind to Al cations over organic ligands (Miyazawa et al. 2013), favouring the formation of SRO constituents (including allophane) rather than that of organo-Al complexes (Percival et al. 2000; Rasmussen et al. 2006; Takahashi et al. 2012). This is also clearly reflected in the PCA results where soil pH positively varied with allophane content and negatively with the ratio of Al_{py}/Al_{ox} (Fig. 5a).

Although the Al_{py}/Al_{ox} ratio was highest in the uppermost layer, peak Al_{py} was reached at a depth of 10–30 cm (Fig. 1e). This can be explained by the fact that the interaction of Al cations with organic moieties is favoured by a certain degree of organic matter processing (i.e. depolymerisation and oxidation) (Kleber et al. 2015; Pérez-Fodich and Derry 2019), and this is not likely to occur in the fresh plant residues that predominate in the uppermost layer. At deeper depths (i.e., below 30 cm), as soil organic C concentrations and soil acidity further decrease (Fig. 2, S2), the formation of SRO constituents is favoured rather than organo-Al complexes, causing a drop in Al_{py}.

It can be argued that the timescales for soil weathering and soil organic C accumulation can differ by orders of magnitude. However, under humid weathering conditions, as observed here, the weathering of volcanic materials could be very rapid. According to a recent study (Anda et al. 2023), the solum developmental rates in pyroclastic deposits were estimated to be 1.2 to 5.3 mm $year^{-1}$, which are faster than that in other parent materials (0.0001 to 0.6 mm $year^{-1}$). A timescale of 200–300 years may be sufficient to form an Andisol from fresh tephra under a humid weathering regime (Delmelle et al. 2015). Such a timescale is relevant for soil C-climate feedback modelling. However, the case can be very different in soils developed from other types of parent materials under different climate regimes.

Temperature influences soil organic composition and C fractions

The effects of temperature on soil organic matter composition, although less evident than the effect of soil depth, are distinguishable and consistent when evaluated at a specific soil layer across the thermal gradient (Figs. 4 and 6). The pyrolysis results clearly support the second hypothesis that soil organic C consists of more plant-derived compounds at colder sites and more microbially-processed products at warmer sites (Fig. 4). Soil carbohydrates predominantly comprise microbial polysaccharides (e.g., furans) and plant polysaccharides (e.g., levoglucosan) (Buurman

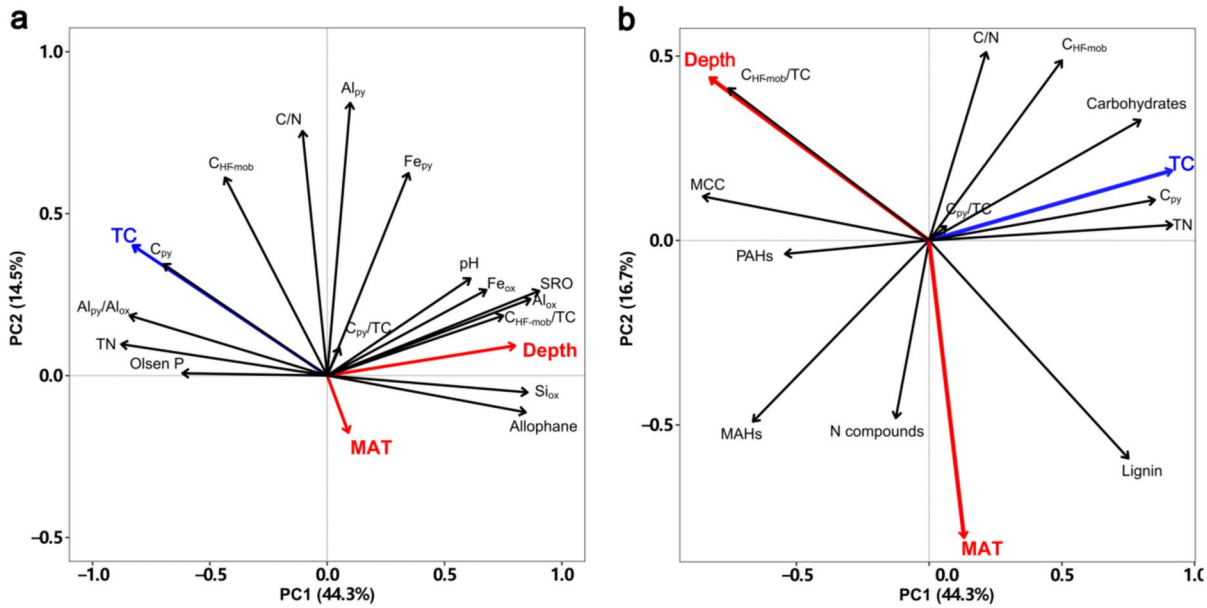

Fig. 5 Principal Component Analysis loadings of geochemical properties and organic composition of soils across the thermal gradient. **a** geochemical properties and **b** soil organic composition assessed by Py-GC/MS. MAT and soil depth are marked in red arrows to highlight their ultimate controls over soil TC (indicated by blue arrows) by regulating the geochemical and organic composition variables (in black arrows). Abbreviations: MAT, mean annual temperature; Al_{py}, Fe_{py} and C_{py} pyrophosphate-extractable Al and Fe, respectively; Al_{ox}, Fe_{ox}, and Si_{ox}, oxalate-extractable Al, Fe and Si, respectively; SRO constituents, $Al_{ox} + 1/2Fe_{ox}$; TC, TN and C/N, total C, total N and C to N ratio, respectively; C_{HF-mob}, 2% hydrofluoric acid mobilised C; C_{py}, pyrophosphate extractable C; MAHs, PAHs and MCC, mono- and poly-aromatic hydrocarbons and methylene chain compounds, respectively

et al. 2007). In the present study, carbohydrates mostly consist of levoglucosan, indicative of the prevailing intact plant remains as their main source rather than microbial polysaccharides. The relative abundance of levoglucosan decreased as temperature increased (data not shown), suggesting that plant-derived carbohydrates are preferentially decomposed at warmer sites. Nitrogen compounds, measured by pyrolysis-GC/MS, have frequently been assigned to microbially-derived soil organic C (Wang et al. 2016; Shen et al. 2018). We expect that the relative abundance of N compounds increased with temperature, implying organic C enriched in microbially-derived compounds at warmer sites. However, this trend is not clearly seen, probably because the HF treatment selectively removes N-rich compounds (Wang et al. 2016). Although lignin is an unequivocal biomarker of plant-derived C (Whalen et al. 2022; Angst et al. 2021), its abundance increased with temperature, which can be explained by the selective preservation of lignin during microbial decomposition of soil organic C by forming mineral-associated C (Huang et al. 2019). Although lignin is usually believed to have a greater intrinsic temperature sensitivity than labile compounds, e.g., carbohydrates, due to its poor quality (Jia et al. 2023), the formation of organo-mineral associations can obscure this intrinsic temperature sensitivity of lignin decomposition (Davidson and Janssens 2006). Collectively, these results demonstrate that soil organic C is more microbially processed at higher temperature than under colder conditions.

The lack of significant difference in the C_{py}/C_{HF-mob} ratio across the thermal gradient (Fig. 3) suggests that the relative importance of metal cation-complexed organic C versus mineral-associated C does not differ with temperature. However, the observation that total C-normalised C_{HF-mob} significantly increased from T7 to T10 (Fig. 3) partly supports the third hypothesis that at warmer sites, a greater proportion of soil organic C was protected by forming mineral-associated C. The increased total C-normalised C_{HF-mob} is

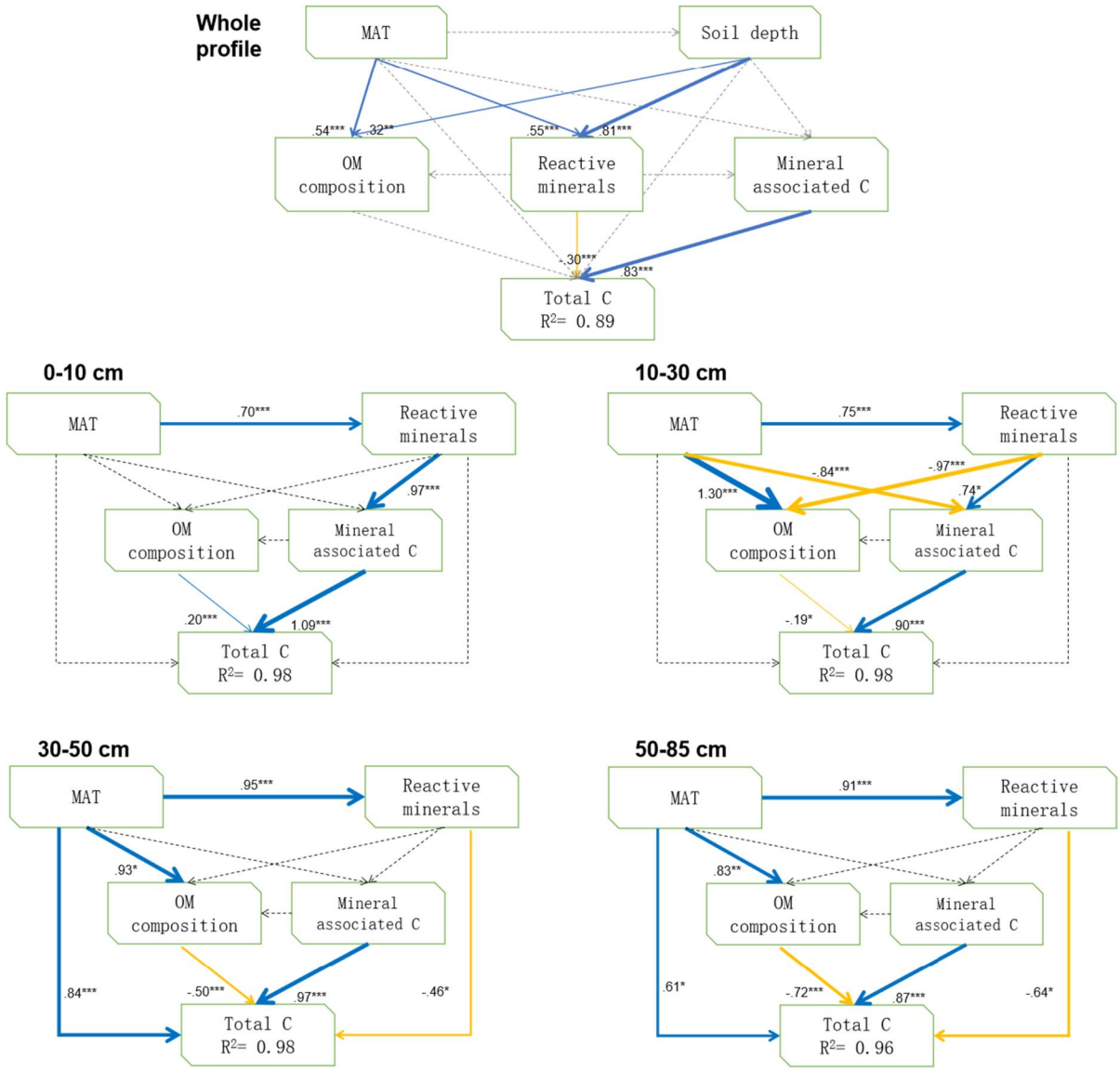

Fig. 6 Structural equation modelling of factors regulating total C contents in soils across the thermal gradient. Mineral-associated C is represented by $C_{HF\text{-}mob}$, reactive minerals primarily by oxalate-extractable ions and SRO constituents, and organic composition largely by N compounds, PAHs and MCCs, respectively. Blue and yellow arrows indicate significant ($P < 0.05$) positive and negative effects, respectively. Grey dotted arrows suggest nonsignificant effects ($P > 0.05$). Significant path coefficients are indicated by numbers and line widths. *, ** and *** indicate significant levels of 0.05, 0.01, and 0.001, respectively

not translated into soil organic C stocks at warmer sites, suggesting that the mineral-associated C is formed at the expense of labile C, as evidenced by the negative relationship between $C_{HF\text{-}mob}$ and plant-derived carbohydrates (Fig. 5b). The results from our structural equation modelling imply that temperature influences soil mineral-associated C primarily via its effects on soil reactive minerals only at 0–30 cm (Fig. 6), while the effect diminishes at deeper soil layers although reactive minerals tend to increase with MAT (Fig. 1, which will be discussed in the next subsection).

The sharp increase with depth in the total C-normalised $C_{HF\text{-}mob}$ is expected and is in line with

previous studies (e.g., Masiello et al. 2004; Rumpel et al. 2006; Eusterhues et al. 2007). This increase in total C-normalised $C_{HF\text{-}mob}$ can be explained by the fact that near the surface, especially in the 0–10 cm layer, there is a greater amount (and proportion) of plant-derived C and a richer abundance of anhydrosugars and other compounds from fresh plant material. This weakly-decomposed (i.e., large molecular weight) and weakly-oxidized C pool (i.e., poor in carboxylic functional groups) is less likely to interact with mineral surfaces than more microbially-processed C (Kleber et al. 2015), which is more abundant at depth. Similar results have also been observed in an umbric Andosol in the Tenerife, Canary Islands (Rumpel et al. 2012). More details on the organo-mineral interactions were revealed by nanoscale secondary ion mass spectrometry (NanoSIMS) in a previous study at the T10 site (Li et al. 2022). The increase in the more microbially-processed C with depth inferred from the abundance of methylene chain compounds (Fig. 4, Naafs et al. 2004) is paralleled by an increase in the reactive sites, which favoured the preservation of C in organo-mineral interactions (Li et al. 2022).

Intricate effects of temperature and soil reactive minerals on soil organic C

Our data clearly indicated that temperature impacted (i) soil reactive Al and Fe (with the reactive Al/Fe transitioning from a greater dominance of metal cations associated with organic ligands at lower temperatures to SRO constituents at higher temperatures), (ii) the soil organic C fractions (with a trend of organic ligands increasingly associated with minerals with increasing temperature), and (iii) soil organic matter composition (with a transition from more plant-derived C to more microbial derived C with increasing temperature). The results of our structural equation modelling also showed that these factors differed in their effects on soil total C depending on soil depth, which confounded the effect of temperature (Fig. 6).

Despite the strong interferences from soil reactive minerals, and soil organic C fractions and composition, temperature stood out as an important regulating factor of soil organic C storage, in particular at 30–85 cm soil depth where MAT had a direct positive effect on total soil C (Fig. 6). Such a positive effect is probably related to an increase in fresh C input at warmer sites. Previous work showed that both annual aboveground and belowground plant carbon inputs increased with MAT across the temperature gradient of Mt. Taranaki (Siregar 2023). Moreover, this assumption is consistent with the finding of Kramer and Chadwick (2016) that C supply is a governing factor of subsoil organic C accumulation in volcanic soils across a thermal gradient on Mauna Kea, Hawaii. The positive effect of MAT on soil total C was partly counteracted by the negative effect of soil organic matter composition (Fig. 6), which is closely associated with microbial-derived compounds (e.g., N compounds and methylene chain compounds, Naafs et al. 2004). Clearly, the negative effect of soil organic matter composition on total C can be interpreted by microbial decomposition of fresh plant C input which leads to the accumulation of microbial-derived compounds. This statement is supported by the positive effect of MAT on soil organic matter composition. More specifically, at low-temperature sites, the colder environment slows down the decomposition of plant C, while decomposition is enhanced at warmer sites.

Surprisingly, soil reactive minerals exerted a negative effect on total soil C at 30–85 cm (Fig. 6), which also partly offset the positive effect of temperature. The negative effect on total soil C seems to contradict previous findings that soil reactive minerals are a primary control over soil organic C storage across a 4000-km-long transect of natural ecosystems in South America (Doetterl et al., 2015) and in a continental-scale soil survey in USA (Rasmussen et al. 2018). The primary control of reactive minerals on total soil C is believed to be derived from the tight interactions between the minerals and the C fractions associated with them. It is the mineral-associated C that determines soil total C in Andosols (Miyazawa et al. 2013; Matus et al. 2014). However, in the present study, at the depth of 30–85 cm, greater abundance of reactive minerals did not increase mineral-associated C (Fig. 6). Similar results have been widely distributed in global subsoils and are attributed to plant C inputs limitations in deep soil layers where plant roots are scarce (Georgiou et al. 2022). In contrast, at the 0–30 cm depth where plant C inputs are plenty, a tight linkage is observed between reactive minerals and mineral-associated C, which in turn benefits soil C storage.

Conclusions

This study disentangles the effects of temperature and reactive minerals on soil organic C across a thermal gradient along the elevational gradient of Mt. Taranaki. From the results obtained, we can infer that fresh C inputs, rather than mineral protection, contribute to maintaining similar soil organic C stocks across the thermal gradient of soils derived from volcanic materials under humid-temperate climatic conditions. This study thus reveals the key role of plant C inputs in mediating soil organic C responses to warming, even in volcanic soils, where mineral-protected C pool is particularly large. Further efforts should be made in future studies to better quantify the impact of temperature on fresh C inputs, particularly under conditions where other factors affecting plant growth are non-limiting.

Author contributions Conceptualisation: MC-A. Formal analysis: IHS, TW, MC-A. Funding acquisition: MC-A, GK. Investigation: IHS, TW. Methodology: IHS, TW, MC-A. Project Administration: MC-A. Visualisation: IHS, TW, MC-A. Supervision: MC-A, TW, MUFK, GK, AP. Writing: IHS and TW, with inputs from all other authors.

Funding This project was financially supported by Massey University core funding. I.S. thanks the support provided by the NZAID Scholarship Program of the New Zealand Ministry of Foreign Affairs and Trade (MFAT). T.W. is grateful for a Start-up Research Grant of the Institute of Mountain Hazards and Environment CAS (E0K2140140) and Sichuan Science and Technology Program (No. 2023NSFSC0190).

Data availability All data generated during this study are presented in the main text and the supporting information and are available upon request from the authors.

Declarations

Conflict of interest The authors declare no conflict of interest to disclose.

References

Aitken JF, Campbell IB, Wilde RH (1978) Soils of Stratford County, North Island, New Zealand. New Zealand Soil Bureau, Department of Scientific and Industrial Research

Anda M, Purwanto S, Dariah A, Watanabe T, Dahlgren RA (2023) A 200-year snapshot of soil development in pyroclastic deposits derived from the 1815 super explosive eruption of Mount Tambora in Indonesia. Geoderma 433:116454

Angst G, Mueller KE, Nierop KG, Simpson MJ (2021) Plant-or microbial-derived? A review on the molecular composition of stabilized soil organic matter. Soil Biol Biochem 156:108189

Blakemore LC (1981) Methods for chemical analysis of soils. Scientific Report 10A New Zealand Soil Bureau

Buurman P, Peterse F, Almendros Martin G (2007) Soil organic matter chemistry in allophanic soils: a pyrolysis-GC/MS study of a Costa Rican Andosol catena. Eur J Soil Sci 58(6):1330–1347. https://doi.org/10.1111/j.1365-2389.2007.00925.x

Carey JC, Tang J, Templer PH, Kroeger KD, Crowther TW, Burton AJ, Dukes JS, Emmett B, Frey SD, Heskel MA, Jiang L, Machmuller MB, Mohan J, Panetta AM, Reich PB, Reinschj S, Wang X, Allison SD, Bamminger C, Tietema A (2016) Temperature response of soil respiration largely unaltered with experimental warming. Proc Natl Acad Sci USA 113(48):13797–13802. https://doi.org/10.1073/pnas.1605365113

Carvalhais N, Forkel M, Khomik M, Bellarby J, Jung M, Migliavacca M, Reichstein M (2014) Global covariation of carbon turnover times with climate in terrestrial ecosystems. Nature 514(7521):213–217

Clarkson BD (1990) A review of vegetation development following recent (<450 years) volcanic disturbance in North Island, New Zealand. NZ J Ecol 14:59–71

Conant RT, Ryan MG, Ågren GI, Birge HE, Davidson EA, Eliasson PE, Evans SE, Frey SD, Giardina CP, Hopkins FM, Hyvönen R, Kirschbaum MUF, Lavallee JM, Leifeld J, Parton WJ, Megan Steinweg J, Wallenstein MD, Martin Wetterstedt JÅ, Bradford MA (2011) Temperature and soil organic matter decomposition rates—synthesis of current knowledge and a way forward. Glob Change Biol 17(11):3392–3404

Cox PM, Pearson D, Booth BB, Friedlingstein P, Huntingford C, Jones CD, Luke CM (2013) Sensitivity of tropical carbon to climate change constrained by carbon dioxide variability. Nature 494(7437):341–344

Crowther TW, Todd-Brown KEO, Rowe CW, Wieder WR, Carey JC, Machmuller MB, Snoek BL, Fang S, Zhou G, Allison SD, Blair JM, Bridgham SD, Burton AJ, Carrillo Y, Reich PB, Clark JS, Classen AT, Dijkstra FA, Elberling B, Bradford MA (2016) Quantifying global soil carbon losses in response to warming. Nature 540(7631):104–108. https://doi.org/10.1038/nature20150

Dahlgren R, Shoji S, Nanzyo M (1993) Mineralogical characteristics of volcanic ash soils. In: Shoji S (ed) Volcanic ash soils genesis, properties and utilization. Elsevier, Amsterdam, pp 101–143

Dahlgren RA, Saigusa M, Ugolini FC (2004) The nature, properties and management of volcanic soils. Adv Agron 82:113–182

Davidson EA, Janssens IA (2006) Temperature sensitivity of soil carbon decomposition and feedbacks to climate change. Nature 440:165–173. https://doi.org/10.1038/nature04514

Davies R, Lambert RE (2015) Under the mountain: how a volcanic peak has influenced the culture, ecology and landscape history of Taranaki, New Zealand

Delmelle P, Opfergelt S, Cornelis J-T, Ping C-L (2015) Chapter 72: volcanic soils. In: Sigurdsson H (ed) The encyclopedia of volcanoes, 2nd edn. Academic Press, Amsterdam, pp 1253–1264

Doetterl S, Stevens A, Six J, Merckx R, Van Oost K, Casanova Pinto M, Casanova-Katny A, Muñoz C, Boudin M, Zagal Venegas E, Boeckx P (2015) Soil carbon storage controlled by interactions between geochemistry and climate. Nat Geosci 8:780–783. https://doi.org/10.1038/ngeo2516

Eusterhues K, Rumpel C, Kleber M, Kögel-Knabner I (2003) Stabilisation of soil organic matter by interactions with minerals as revealed by mineral dissolution and oxidative degradation. Org Geochem 34(12):1591–1600

Eusterhues K, Rumpel C, Kögel-Knabner I (2007) Composition and radiocarbon age of HF-resistant soil organic matter in a Podzol and a Cambisol. Org Geochem 38(8):1356–1372. https://doi.org/10.1016/j.orggeochem.2007.04.001

Friedlingstein P, Cox P, Betts R, Bopp L, von Bloh W, Brovkin V, Cadule P et al (2006) Climate–carbon cycle feedback analysis: results from the C4MIP model intercomparison. J Clim 19:3337–3353

Georgiou K, Jackson RB, Vindušková O, Abramoff RZ, Ahlström A, Feng W, Harden JW, Pellegrini AFA, Polley HW, Soong JL, Riley WJ, Torn MS (2022) Global stocks and capacity of mineral-associated soil organic carbon. Nat Commun 13(1):3797

Giardina CP, Litton CM, Crow SE, Asner GP (2014) Warming-related increases in soil CO_2 efflux are explained by increased below-ground carbon flux. Nat Clim Chang 4(9):822–827

Hashizume H, Theng BKG (2007) Adenine, adenosine, ribose and 5′-AMP adsorption to allophane. Clays Clay Miner 55(6):599–605. https://doi.org/10.1346/CCMN.2007.0550607

Hicks Pries CE, Castanha C, Porras RC, Torn MS (2017) The whole-soil carbon flux in response to warming. Science 355(6332):1420–1423

Huang W, Hammel KE, Hao J, Thompson A, Timokhin VI, Hall SJ (2019) Enrichment of lignin-derived carbon in mineral-associated soil organic matter. Environ Sci Technol 53(13):7522–7531

IPCC (2021) Climate change 2021: the physical science basis. Contribution of working group I to the sixth assessment report of the intergovernmental panel on climate change. Cambridge University Press, Cambridge, United Kingdom and New York, NY, USA

Jia J, Liu Z, Haghipour N, Wacker L, Zhang H, Sierra CA, Ma T, Wang Y, Chen L, Luo A, Wang Z, He J-S, Zhao M, Eglinton TI, Feng X (2023) Molecular 14C evidence for contrasting turnover and temperature sensitivity of soil organic matter components. Ecol Lett 26(5):778–788

Jones RJA, Hiederer R, Rusco E, Montanarella L (2005) Estimating organic carbon in the soils of Europe for policy support. Eur J Soil Sci 56(5):655–671. https://doi.org/10.1111/j.1365-2389.2005.00728.x

Keesstra SD, Bouma J, Wallinga J, Tittonell P, Smith P, Cerdà A, Fresco LO (2016) The significance of soils and soil science towards realization of the United Nations sustainable development goals. Soil 2(2):111–128. https://doi.org/10.5194/soil-2-111-2016

Kirschbaum MUF (2000) Will changes in soil organic matter act as a positive or negative feedback on global warming? Biogeochemistry 48:21–51. https://doi.org/10.1023/A:1006238902976}

Kleber M, Eusterhues K, Keiluweit M, Mikutta C, Mikutta R, Nico PS (2015) Mineral–organic associations: formation, properties, and relevance in soil environments. Adv Agron 130:1–140

Kramer MG, Chadwick OA (2016) Controls on carbon storage and weathering in volcanic soils across a high-elevation climate gradient on Mauna Kea, Hawaii. Ecology 97(9):2384–2395

Lawrence CR, Schulz MS, Masiello CA, Chadwick OA, Harden JW (2021) The trajectory of soil development and its relationship to soil carbon dynamics. Geoderma 403:115378

Li J, Nie M, Pendall E, Reich PB, Pei J, Noh NJ, Zhu T, Li B, Fang C (2020) Biogeographic variation in temperature sensitivity of decomposition in forest soils. Glob Change Biol 26(3):1873–1885

Li Y, Camps-Arbestain M, Whitby CP, Wang T, Mueller CW, Hoeschen C, Beare MH (2022) Functional complexity explains the depth-dependent response of organic matter to liming at the nanometer scale. Geoderma 408:115560. https://doi.org/10.1016/j.geoderma.2021.115560

Macías F, Camps-Arbestain M (2020) A biogeochemical view of the world reference base soil classification system: homage to Ward Chesworth. In: Sparks DL (ed) Advances in agronomy. Springer, New York, pp 295–342

Masiello CA, Chadwick OA, Southon J, Torn MS, Harden JW (2004) Weathering controls on mechanisms of carbon storage in grassland soils. Glob Biogeochem Cycles 18(4):G4023

Matus F, Rumpel C, Neculman R, Panichini M, Mora ML (2014) Soil carbon storage and stabilisation in andic soils: a review. CATENA 120:102–110

McGlone MS, Neall VE, Clarkson BD (1988) The effect of recent volcanic events and climatic changes on the vegetation of Mt. Egmont (Mt. Taranaki), New Zealand. N Z J Bot 26(1):123–144. https://doi.org/10.1080/0028825X.1988.10410105

Melillo JM, Frey SD, DeAngelis KM, Werner WJ, Bernard MJ, Bowles FP, Pold G, Knorr MA, Grandy AS (2017) Long-term pattern and magnitude of soil carbon feedback to the climate system in a warming world. Science 358(6359):101–105

Miyazawa M, Takahashi T, Sato T, Kanno H, Nanzyo M (2013) Factors controlling accumulation and decomposition of organic carbon in humus horizons of Andosols: a case study for distinctive non-allophanic Andosols in northeastern

Japan. Biol Fertil Soils 49(7):929–938. https://doi.org/10.1007/s00374-013-0792-8
Mizota C, Van Reeuwijk LP (1989) Clay mineralogy and chemistry of soils formed in volcanic material in diverse climatic regions. International Soil Reference and Information Centre (ISRIC)
Naafs DF, van Bergen PF, Boogert SJ, de Leeuw JW (2004) Solvent-extractable lipids in an acid andic forest soil; variations with depth and season. Soil Biol Biochem 36(2):297–308
Parfitt RL (2009) Allophane and imogolite: role in soil biogeochemical processes. Clay Miner 44(1):135–155. https://doi.org/10.1180/claymin.2009.044.1.135
Percival HJ, Parfitt RL, Scott NA (2000) Factors controlling soil carbon levels in New Zealand grasslands: Is clay content important? Soil Sci Soc Am J 64(5):1623–1630. https://doi.org/10.2136/sssaj2000.6451623x
Perez-Fodich A, Derry LA (2019) Organic acids and high soil CO_2 drive intense chemical weathering of Hawaiian basalts: insights from reactive transport models. Geochim Cosmochim Acta 249:173–198
Rasmussen C, Southard RJ, Horwath WR (2006) Mineral control of organic carbon mineralisation in a range of temperate conifer forest soils. Glob Change Biol 12(5):834–847. https://doi.org/10.1111/j.1365-2486.2006.01132.x
Rasmussen C, Heckman K, Wieder WR, Keiluweit M, Lawrence CR, Berhe AA, Wagai R (2018) Beyond clay: towards an improved set of variables for predicting soil organic matter content. Biogeochemistry 137:297–306
Rumpel C, Rabia N, Derenne S, Quenea K, Eusterhues K, Kögel-Knabner I, Mariotti A (2006) Alteration of soil organic matter following treatment with hydrofluoric acid (HF). Org Geochem 37(11):1437–1451
Rumpel C, Chaplot V, Chabbi A, Largeau C, Valentin C (2008) Stabilisation of HF soluble and HCl resistant organic matter in sloping tropical soils under slash and burn agriculture. Geoderma 145(3):347–354
Rumpel C, Rodríguez-Rodríguez A, González-Pérez JA, Arbelo C, Chabbi A, Nunan N, González-Vila FJ (2012) Contrasting composition of free and mineral-bound organic matter in top-and subsoil horizons of Andosols. Biol Fertil Soils 48:401–411
Schwager SJ, Mikhailova EA (2002) Estimating variability in soil organic carbon storage using the method of statistical differentials. Soil Sci 167(3):194–200
Shen Q, Suarez-Abelenda M, Camps-Arbestain M, Calvelo Pereira R, McNally SR, Kelliher FM (2018) An investigation of organic matter quality and quantity in acid soils as influenced by soil type and land use. Geoderma 328:44–55. https://doi.org/10.1016/j.geoderma.2018.05.006
Siregar I (2023) An investigation of soil carbon fluxes and pools in the thermo-sequence of Mt. Taranaki forest. PhD thesis, Massey University, NZ
Suárez-Abelenda M, Ahmad R, Camps-Arbestain M, Herath SHMSK (2015) Changes in the chemical composition of soil organic matter over time in the presence and absence of living roots: a pyrolysis GC/MS study. Plant Soil 391(1–2):161–177. https://doi.org/10.1007/s11104-015-2423-7
Takahashi T, Dahlgren RA (2016) Nature, properties and function of aluminum–humus complexes in volcanic soils. Geoderma 263:110–121. https://doi.org/10.1016/j.geoderma.2015.08.032
Takahashi T, Kanno H, Nanzyo M (2012) Factors affecting organic carbon accumulation in humus horizons of volcanic soils from the Tohoku University World Andosol Database: a path analysis. Pedologist 56(2):58–62. https://doi.org/10.18920/pedologist.56.2_58
Tian Y, Schindlbacher A, Malo CU, Shi C, Heinzle J, Kwatcho Kengdo S, Inselsbacher E, Borken W, Wanek W (2023) Long-term warming of a forest soil reduces microbial biomass and its carbon and nitrogen use efficiencies. Soil Biol Biochem 184:109109
Torres-Orozco R, Cronin SJ, Damaschke M, Pardo N (2017) Diverse dynamics of Holocene mafic-intermediate Plinian eruptions at Mt. Taranaki (Egmont), New Zealand. Bull Volcanol 79(11):1–27
Trumbore SE, Czimczik CI (2008) An uncertain future for soil carbon. Science 321(5895):1455–1456
Wang T, Camps-Arbestain M, Hedley C (2016) Factors influencing the molecular composition of soil organic matter in New Zealand grasslands. Agr Ecosyst Environ 232:290–301. https://doi.org/10.1016/j.agee.2016.08.016
Wendt JW, Hauser S (2013) An equivalent soil mass procedure for monitoring soil organic carbon in multiple soil layers. Eur J Soil Sci 64(1):58–65. https://doi.org/10.1111/ejss.12002
Whalen ED, Grandy AS, Sokol NW, Keiluweit M, Ernakovich J, Smith RG, Frey SD (2022) Clarifying the evidence for microbial-and plant-derived soil organic matter, and the path toward a more quantitative understanding. Glob Change Biol 28(24):7167–7185
World Reference Base for Soil Resources (2015) World reference base for soil resources, update 2015. World Soil Resources Reports No. 106.FAO
Xu W, Yuan W, Cui L, Ma M, Zhang F (2019) Responses of soil organic carbon decomposition to warming depend on the natural warming gradient. Geoderma 343:10–18. https://doi.org/10.1016/j.geoderma.2019.02.017
Yuan G, Theng BKG, Parfitt RL, Percival HJ (2000) Interactions of allophane with humic acid and cations. Eur J Soil Sci 51(1):35–41
Zegouagh Y, Derenne S, Dignac MF, Baruiso E, Mariotti A, Largeau C (2004) Demineralisation of a crop soil by mild hydrofluoric acid treatment: influence on organic matter composition and pyrolysis. J Anal Appl Pyrolysis 71(1):119–135